International Journal of Multiphase Flow 35 (2009) 323–334

Contents lists available at ScienceDirect

International Journal of Multiphase Flow

journal homepage: www.elsevier.com/locate/ijmulflow

Benchmarking of the one-dimensional one-group interfacial area transport equation for reduced-gravity bubbly flows

S. Vasavada [a,*], X. Sun [b], M. Ishii [a], W. Duval [c]

[a] School of Nuclear Engineering, Purdue University, 400 Central Drive, West Lafayette, IN 47907, USA
[b] Department of Mechanical Engineering, The Ohio State University, 201 West 19th Avenue, Columbus, OH 43210, USA
[c] Fluid Physics and Transport Branch, NASA Glenn Research Center, 21000 Brookpark Road, Cleveland, OH 44135, USA

ARTICLE INFO

Article history:
Received 16 September 2008
Received in revised form 10 December 2008
Accepted 18 January 2009
Available online 4 February 2009

Keywords:
Liquid-liquid flow
Reduced gravity
Interfacial area
Coalescence
Disintegration
Two-phase flow

ABSTRACT

In order to properly design and safely operate two-phase flow systems, especially those deployed on future space missions, it is necessary to have accurate predictive capabilities. The application of a novel predictive method, the interfacial area transport equation (IATE), to dynamically predict the change of interfacial area concentration for reduced-gravity two-phase flows is described in this paper. Fluid particle interaction mechanisms such as coalescence and breakup that are present in reduced-gravity two-phase flows have been studied experimentally as reported in a previous paper by the current authors [Vasavada et al., 2007]. These mechanisms represent the source and sink terms in the IATE and their mechanistic models are benchmarked using experimental data obtained in a 25 mm inner diameter ground-based test section wherein reduced-gravity conditions were simulated. The comparison of the predictions from the model against experimental data shows good agreement. It has been found that, in contrast to the hypothesis extended in the literature, the wake entrainment based coalescence mechanism is present in reduced-gravity two-phase flows and in some cases is more important than coalescence due to random collision. Physics based arguments are extended to support this conclusion.

1. Introduction

A major issue in current spacecrafts is the efficient removal of heat generated by the crew and equipment onboard thereby ensuring an acceptable environment for life support of the crew and for optimal operation of the equipment. Although heat removal in current spacecrafts is accomplished by using forced convection single-phase liquid loops termed active thermal control systems (ATCSs), future spacecrafts will require higher capacity and more efficient heat removal systems in order to manage the increased heat load (Grigoriev et al., 1996). This can only be realized by using two-phase flow which utilizes the latent heat of evaporation. In view of the advantages to be derived from such a system, a number of researchers (Keshock, 1987; Takamasa et al., 2004, among others) have performed experimental and theoretical studies of two-phase flows under reduced-gravity conditions. Experiments have been carried out for adiabatic and boiling two-phase flows under such conditions using a drop tower, parabolic flights and sounding-rockets to investigate the influence of forces due to surface tension, inertia and gravity on two-phase flow dynamics. Zhao et al. (2001) have studied two-phase flow patterns in actual microgravity conditions based on experiments performed aboard the MIR space station.

For the optimal design and operation of two-phase flow loops for use in space-based systems, it is necessary to accurately model and predict the flow behavior in such two-phase flow systems. A practical approach for prediction would be the development of a two-phase flow analysis code under reduced-gravity conditions. Such codes have been developed for two-phase flow under normal-gravity environment and are currently in use in the field of nuclear engineering where constraints similar to those in a space-based two-phase flow system occur. Such codes, in general, use the two-fluid model to predict the two-phase flow behavior given the initial and boundary conditions.

The two-fluid model is based on two sets of conservation equations governing the balance of mass, momentum, and energy of each phase (Ishii and Hibiki, 2006). The interfacial transfer terms in the conservation equations couple the transport of mass, momentum, and energy of each phase across the interface. In particular, for two-phase flows under reduced-gravity condition, the stability of the fluid particle interface and therefore the interfacial structures are quite different from those under normal-gravity condition (Colin et al., 1991; Vasavada et al., 2007). As a result, the flow structure may not reach an equilibrium condition and the two fluids may be loosely coupled such that each fluid should be considered separately as is done by the two-fluid model.

* Corresponding author. Present address: Energy Research, Inc., 6189 Executive Blvd., Rockville, MD 20852, USA. Tel.: +1 7653463516.
E-mail addresses: svasavad@purdue.edu, sxv@eri-world.com (S. Vasavada), sun.200@osu.edu (X. Sun), ishii@purdue.edu (M. Ishii), Walter.M.Duval@grc.nasa.gov (W. Duval).

0301-9322/$ - see front matter © 2009 Elsevier Ltd. All rights reserved.
doi:10.1016/j.ijmultiphaseflow.2009.01.006

The phase-interaction terms in the two-fluid model can be expressed as a product of the interfacial area concentration and the driving force for the transfer. The interfacial area concentration is one of the important geometrical scales of the flow. Mathematically, it is defined as the interfacial area per unit mixture volume and has the inverse unit of length. The use of an interfacial area transport equation (IATE) has been proposed (Kocamustafaogullari and Ishii, 1995) to dynamically predict the change in interfacial area concentration. In the IATE, generation and destruction of interfacial area are modeled based on fluid particle (e.g., bubbles or droplets) coalescence and disintegration as well as bubble nucleation, evaporation and condensation. These mechanisms are physically responsible for the formation or destruction of fluid particles as well as their increase or decrease in size thereby changing the interfacial area. The IATE can replace the traditional regime transition criteria based approach and complement the two-fluid model (TFM) to provide accurate and dynamic predictions of two-phase flow evolution. Thus, a successful development of the IATE can make a quantum improvement in the TFM formulation. From this point of view, continuous efforts have been made to develop the IATE under normal-gravity environment (Hibiki and Ishii, 1999; Wu et al., 1998; Kim, 1999; Sun, 2001).

For reduced-gravity gas–liquid two-phase flows, however, there are only limited data available in the literature, obtained from either parabolic flights and drop-tower experiments or ground-based simulations. Therefore, it is a challenging task to develop empirical models that can work over a wide range of operation conditions for such flows, including the gravity level, flow rates, system pressure, and temperature. More importantly, even if such models/correlations are developed for reduced-gravity two-phase flows, their applicability to actual conditions in space remains an open question since the flow regime based approach has difficulties in dynamically characterizing the flow transition and development. Therefore, based on the expertise developed and the advantage derived in the normal-gravity gas–liquid two-phase flows, an effort was undertaken to adapt the IATE for the reduced-gravity two-phase flows. In relation to the formulation of the IATE in bubbly flow under reduced-gravity environment, this study aims at developing reliable constitutive relations for the IATE.

The current focus is on modeling coalescence and disintegration of fluid particles, such as bubbles and/or droplets.[1] It should be noted that to develop a transport equation applicable to a wide range of two-phase flows, the differences in the shape and size of bubbles and in the resulting characteristic transport phenomena should be accounted for. In this paper, however, only bubbly flows with spherical bubbles and three interaction mechanisms are being considered. These interaction mechanisms are fluid particle coalescence due to the random motion driven by the turbulent eddies in the continuous phase, coalescence due to the wake entrainment effect, and disintegration due to the impact of turbulent eddies. In addition to providing an accurate predictive tool for reduced-gravity two-phase flow systems the current study has demonstrated the applicability of the IATE to liquid–liquid systems.

The basic formulation of the IATE and some information on the modeling performed for normal-gravity air–water flows for closure of the IATE will be provided in the next section. This will be followed by a brief description of the experimental study and a summary of the experimental results given in Vasavada et al. (2007). The modeling performed for reduced-gravity two-phase flows will be discussed and the predictions of the resulting IATE will be compared against the experimental data. The interpretation of these results will be carried out along with comments on the differences that exist in the current simulation with respect to air–water flows in reduced-gravity conditions.

[1] Henceforth the term "bubble(s)" will be used for both gas bubbles as well as liquid drops. Moreover, the term "fluid particles" should be understood as referring to both bubbles and drops.

2. Formulation of the interfacial area transport equation

The interfacial area transport equation can be derived by considering the fluid particle number density transport equation analogous to the Boltzmann equation (Kocamustafaogullari and Ishii, 1995). By multiplying the bubble number density transport equation by the surface area "carried" by one bubble and then integrating the resulting transport equation over all the possible bubble volumes, a three-dimensional IATE is derived (Ishii and Hibiki, 2006). For some two-phase flow systems, a one-dimensional formulation of the IATE is sufficient to describe the flow behavior. Applying cross-sectional area-averaging to the three-dimensional IATE results in the one-dimensional IATE as:

$$\frac{\partial\langle a_i\rangle}{\partial t}+\frac{\partial}{\partial z}(\langle a_i\rangle\langle\langle v_i\rangle\rangle)=\frac{1}{3\psi}\frac{\langle\alpha\rangle^2}{\langle a_i\rangle}(\phi_B-\phi_C+\phi_P)+\frac{2\langle a_i\rangle}{3\langle\alpha\rangle}\left\{\frac{\partial\langle a_i\rangle}{\partial t}+\frac{\partial}{\partial z}(\langle\alpha\rangle\langle\langle v_g\rangle\rangle)\right\} \quad (1)$$

which can be written as,

$$\frac{\partial\langle a_i\rangle}{\partial t}+\frac{\partial}{\partial z}(\langle a_i\rangle\langle\langle v_i\rangle\rangle)=\Phi_B-\Phi_C+\Phi_P+\Phi_V \quad (2)$$

where,

$$\Phi_j=\frac{1}{3\psi}\frac{\langle\alpha\rangle^2}{\langle a_i\rangle}\phi_j,\Phi_V=\frac{2\langle a_i\rangle}{3\langle\alpha\rangle}\left\{\frac{\partial a_i}{\partial t}+\frac{\partial}{\partial z}(\langle\alpha\rangle\langle\langle v_g\rangle\rangle)\right\}. \quad (3)$$

where $j=B,C$ and P. In the above equations, the symbols a_i, t, v_g, z, ψ and α denote the interfacial area concentration, time, bubble velocity, axial position, a factor depending on the bubble shape ($\psi=\frac{1}{36\pi}$ for spherical bubbles) and the void fraction, respectively. ϕ_B, ϕ_C and ϕ_P are the rates of change of bubble number density due to bubble breakup, bubble coalescence and phase change, respectively. Φ_B, Φ_C, Φ_P and Φ_V are the above three corresponding rates of change of the interfacial area concentration and the change rate due to dispersed phase volume change. Under no phase change condition, ϕ_P and Φ_P become zero. The sink and source terms of the interfacial area concentration, Φ_B and Φ_C, need to be modeled mechanistically based on coalescence and breakup mechanisms. Furthermore, the symbols $\langle\rangle$ and $\langle\langle\rangle\rangle$ represent the area-averaging and void-weighted area-averaging, respectively; and z is the coordinate along the flow direction. The area-averaging of any parameter F can be written mathematically as,

$$\langle F\rangle=\frac{\int_0^A F dA}{A}, \quad (4)$$

where A is the cross-sectional area of the channel and the void-weighted area-averaging can be expressed as,

$$\langle\langle F\rangle\rangle=\frac{\langle\alpha F\rangle}{\langle\alpha\rangle}. \quad (5)$$

It is worthwhile to note at this point that Kamp et al. (2001) have developed a predictive method for reduced-gravity two-phase flows employing moments of bubble diameter instead of the interfacial area concentration arguing that their approach is simpler as compared to the current one. The Sauter mean diameter (D_{sm}) of a bubble/drop and the interfacial area concentration are related to each other as,

$$\langle D_{sm}\rangle=6\frac{\langle\alpha\rangle}{\langle a_i\rangle}. \quad (6)$$

However, the current approach is more general since the diameter of bubbles has true physical significance only for spherical or slightly distorted bubbles. Indeed, this is the range of bubble diam-

eters to which Kamp et al. (2001) have restricted their model validation. The interfacial area concentration, on the other hand, is a geometric parameter that describes, given a certain driving force, the interfacial transfer capability and maintains its physical interpretation regardless of the flow structure. The IATE, therefore, is a more general predictive approach, which can be used for flow conditions consisting of different bubble sizes and shapes. For normal-gravity air–water flows the generality of the IATE has been demonstrated (Kim, 1999; Fu, 2001; Sun, 2001).

For two-phase flows in general, it has been established that the size of the bubbles plays an important role in determining the different kinds of interaction mechanisms that the bubbles experience (Wu et al., 1998; Kim, 1999; Sun et al., 2004b). As a result, during the formulation of the IATE, the bubbles are classified into two groups. For normal gravity air–water flows, Group 1 include the spherical and distorted bubbles while cap shaped, slug (Taylor) and churn-turbulent (highly irregular shaped) bubbles form Group 2. The maximum distorted bubble diameter (introduced in Section 3) is considered as the limit for determining the group that a bubble belongs to Ishii and Hibiki (2006). Details of the development of the two-group IATE for normal-gravity two-phase flows can be found in Fu (2001), Sun et al. (2004a) and Sun et al. (2004b). As will be explained later, since the flow conditions under consideration in the present case are in the bubbly flow and transition from bubbly to slug flow, the drops do not exceed the maximum distorted bubble limit for the current system. Therefore, only the one-group IATE will be explained in detail in the next paragraphs.

For the normal-gravity one-group IATE, the bubble interaction terms were modeled by Wu et al. (1998) and Kim (1999), among others. In the modeling, three bubble interaction mechanisms were considered, namely, bubble disintegration due to turbulent impact (TI), bubble coalescence through random collision driven by the surrounding liquid turbulent eddies (RC), and bubble coalescence due to the wake entrainment of the following bubbles by a preceding bubble (WE). These three processes are depicted pictorially in Fig. 1. The approach for mechanistically modeling these interaction mechanisms is given in Wu et al. (1998). Later it was shown that the bubble expansion (EXP) due to decrease in local pressure on the bubble interface as it rises in an upward two-phase flow can contribute significantly to the interfacial area transport in a relatively low pressure system (Kim, 1999; Hibiki and Ishii, 2000) and this term was incorporated into the formulation.

As mentioned earlier, Φ_{TI}, Φ_{RC}, Φ_{WE} and Φ_{EXP} are the interfacial area concentration source rate due to breakup caused by turbulent impact, sink rates due to coalescence on account of random collision and wake entrainment, and source rate due to the expansion, respectively. Their final forms are given as (Kim, 1999; Hibiki and Ishii, 2000),

$$\Phi_{TI} = C_{TI}\frac{\langle\alpha\rangle^2}{\langle a_i\rangle^2}\left(\frac{12\pi n u_t}{\langle D_b\rangle}\right)\exp\left(-\frac{We_{crit}}{We}\right)\sqrt{1-\frac{We_{crit}}{We}}, \tag{7}$$

$$\Phi_{RC} = C_{RC}\frac{\langle\alpha\rangle^2}{\langle a_i\rangle^2}\left(\frac{12\pi n^2 u_t\langle D_b\rangle^2}{\langle\alpha_{max}\rangle^{1/3}}\left(\langle\alpha\rangle^{1/3}-\langle\alpha_{max}\rangle^{1/3}\right)\right) \times\left(1-\exp\left(-C\frac{\langle\alpha_{max}\rangle^{1/3}\langle\alpha\rangle^{1/3}}{\left(\langle\alpha\rangle^{1/3}-\langle\alpha_{max}\rangle^{1/3}\right)}\right)\right), \tag{8}$$

$$\Phi_{WE} = 12\pi C_{WE}C_D^{1/3}n^2\langle D_b\rangle^2\langle u_r\rangle\frac{\langle\alpha\rangle^2}{\langle a_i\rangle^2}, \tag{9}$$

$$\Phi_{EXP} = \frac{2\langle a_i\rangle}{3\langle\alpha\rangle}\left\{\frac{\partial\langle\alpha\rangle}{\partial t}+\frac{\partial}{\partial z}\left(\langle\alpha\rangle\langle\langle v_g\rangle\rangle\right)\right\}. \tag{10}$$

In Eqs. (7–9), $C, C_{TI}, C_{RC}, C_{WE}$ are coefficients in the models and are determined experimentally; n, u_t, u_r and D_b are the bubble number density, average turbulent fluctuating velocity, relative velocity between the two phases, and average bubble diameter, respectively; α_{max} is the void fraction of maximum packing limit for spherical bubbles; C_D is the drag coefficient of a bubble of diameter D_b; and We is the Weber number defined as,

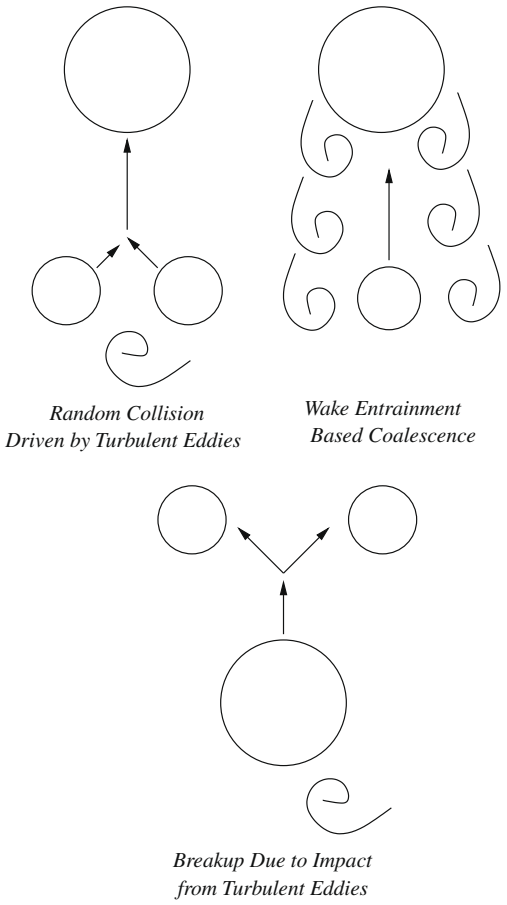

Fig. 1. Schematic representation of important fluid particle interaction mechanisms considered in the development of the one-group IATE.

$$We = \frac{\rho_c u_r^2 D_b}{\sigma} \tag{11}$$

where, ρ_c is the density of the continuous phase and σ is the interfacial tension between the fluids. We_{crit} in Eq. (7) is the critical Weber number. If the Weber number is larger than the critical value, the turbulent impact mechanism may occur. Hence, the turbulent impact mechanism and its model represented by Eq. (7) is of importance only if the condition $We/We_{crit} \geqslant 1$ is met. These relations are used in Eq. (1). Moreover, for quasi-steady two-phase flows, the term with the time derivative is dropped. In addition, for adiabatic flows like those in the current study, the phase change term in Eq. (1) is also neglected. The final form of the one-dimensional, steady-state, adiabatic, one-group IATE with interaction terms modeled for normal-gravity air–water flows is,

$$\begin{aligned}\frac{d\langle a_i\rangle\langle\langle v_{gz}\rangle\rangle}{dz} &= \left(\frac{2\langle a_i\rangle\langle\langle v_{gz}\rangle\rangle}{\langle p\rangle}\right)\left(-\frac{d\langle p\rangle}{dz}\right) \\ &+\frac{C_{TI}}{18}\left(\frac{\langle a_i\rangle^2\langle u_t\rangle}{\langle\alpha\rangle}\right)\sqrt{1-\frac{We_{crit}}{We}}\exp\left(-\frac{We_{crit}}{We}\right) \\ &-\frac{C_{RC}}{3\pi}\frac{\langle a_i^2\rangle\langle u_t\rangle}{\langle\alpha_{max}\rangle^{\frac{1}{3}}\left(\langle\alpha_{max}\rangle^{\frac{1}{3}}-\langle\alpha\rangle^{\frac{1}{3}}\right)} \\ &\times\left(1-exp\left(-C\frac{\langle\alpha\rangle^{\frac{1}{3}}\langle\alpha_{max}\rangle^{\frac{1}{3}}}{\langle\alpha_{max}\rangle^{\frac{1}{3}}-\langle\alpha\rangle^{\frac{1}{3}}}\right)\right)-\frac{C_{WE}C_D^{\frac{1}{3}}}{3\pi}\langle a_i\rangle^2\langle u_r\rangle,\end{aligned} \tag{12}$$

where, the bubble number density n and the bubble diameter D_b were treated as,

$$n = \frac{\langle a_i \rangle^3}{36\pi\langle\alpha\rangle^2}, \langle D_b \rangle \approx \langle D_{sm} \rangle = \frac{6\langle\alpha\rangle}{\langle a_i \rangle}. \quad (13)$$

In Eq. (12), the ideal gas law is used to determine the gas density resulting in the first term on the RHS and v_{gz} is the local dispersed phase velocity at an axial location. It should be noted that the covariance terms resulting from the area-averaging process were neglected in view of the fact that the profiles of a_i, α and v_{gz} were nearly uniform across the pipe cross-section in most of the current flow conditions (Vasavada et al., 2007). This is true for reduced-gravity two-phase flows in general where the reduction in relative velocity due to a decrease in buoyancy decreases the effect of lateral forces on the phase distribution (Colin et al., 1993; Kamp et al., 1995). Moreover, the size of bubbles under such conditions is significantly large as compared to normal-gravity two-phase flows (see next section) and therefore offers more resistance to motion towards the channel center or wall. Further, droplet center of mass velocity is assumed to be equal to the interfacial velocity which is a valid assumption for most practical two-phase flow systems including the current one.

3. Experimental study

To gain a better understanding of reduced-gravity two-phase flow and to aid the modeling effort, a ground-based experiment program has been developed (Vasavada et al., 2007). In the study, a reduced-gravity condition is simulated in a 25 mm inner diameter (ID) test section on ground using two immiscible liquids of similar density, namely, water as the continuous phase (density: 998.2 kg/m^3 at 20 °C and 1 atm) and Therminol 59® as the dispersed phase (density: 970 kg/m^3 at the same state). This effectively reduces the body force effect, which is the most dominant influence of the gravity field on two-phase flow behaviors. Detailed experimental data of the lateral distributions of the void fraction, interfacial area concentration, and bubble velocity for a total of ten flow conditions have been acquired using miniature multi-sensor conductivity probes (Kim et al., 2000). These flow conditions lie in the bubbly and bubbly to slug flow transition regimes and have area-averaged void fractions from 3% to 30% and channel Reynolds number for the continuous phase (Re_c) from 2900 to 8800. In this paper, these experimental data are used to model the interation mechanisms to be included in the IATE applicable to reduced-gravity conditions. Predictions from the model have also been compared against the experimental data. It should be pointed out that the experimental data presented in Vasavada et al. (2007) also compares well with the data taken aboard parabolic flights by other researchers (Dukler et al., 1988; Colin et al., 1991, 1996). The details of the experimental facility and measurement technique are available in Vasavada et al. (2007). Only the important observations from the analysis of the experimental data are summarized hereunder.

As part of the scaling study which was undertaken prior to the experimentation it was found that the internal length scales, which scale the drop/bubble sizes, are large for reduced-gravity cases. As a result, the classification of bubbles/drops into two different groups was different as compared to the normal-gravity case. For the IATE developed for normal-gravity conditions the maximum distorted drop diameter is taken as the limit between Group 1 and Group 2 drops since beyond this size the bubbles change shape and become cap shaped. This also changes the interaction mechanisms that such bubbles participate in. However, for reduced-gravity cases the distorted bubble/drop diameter can be much larger than the channel diameter. Therefore, as the drops reach the size of the channel, the effect of the wall will be prominent in squeezing such drops in the axial direction and changing their shape. Hence the limit for considering the drops to belong to Group 1 or Group 2 in the present case is considered to be a function of the hydraulic diameter of the channel. According to Clift et al. (1978), the effect of the wall on the shape of bubbles/drops starts to become prominent at $\sim 0.7D_h$. Govier and Aziz (1972) consider the transition from cap-bubbly flow to slug flow in pipes occurs when the cap bubble base length reaches $0.75D_h$. Therefore, in the present case the demarcation between Group 1 and Group 2 drops is chosen to be $0.75D_h$. These arguments will also be valid for gas–liquid flow in actual reduced-gravity conditions where the distorted bubble/drop limit is larger than the channel size.

However, it is also recognized that for Group 1 drops, as they increase in size beyond half the channel diameter, the lateral interactions will become increasingly improbable. For the flow conditions that have been validated and the results for which will be discussed in this paper, only two flow conditions lying close to the transition boundary from bubbly to slug flow (Runs 6 and 7, see Table 1) had drop Sauter mean diameters close to the maximum distorted limit (please note that the limit was never crossed for any flow condition presented here). Characteristic images for Runs 5, 7 and 9 taken using a high-speed video camera at an $L/D_h \sim 42$ are shown in Fig. 2 to support this assertion. Since the distortion of the drops, based on flow visualization, was not found to be significant, the drops in Runs 6 and 7 were categorized as Group 1 drops. Hence, the reduction in the probability for lateral interactions between distorted drops is not accounted for in the present study. This will be taken into account while modeling the two-group IATE for reduced-gravity conditions. Development and evaluation of the two-group IATE are the next steps in the research program and the results of the same will be reported in the literature.

The ten flow conditions for which local data have been acquired are shown on a flow pattern map (in the parametric space of continuous phase and dispersed phase volumetric flux, j_c and j_d, respectively) in Fig. 3. The bubbly to slug flow transition line given by Mishima and Ishii (1984) is also shown in Fig. 3 to provide the positions of the ten flow conditions relative to the transition line. The validity of transition criterion given by Mishima and Ishii (1984) in predicting the transition from bubbly to slug flow for reduced-gravity two-phase flows has been shown in Vasavada et al. (2007). It should be noted that in the remainder of this paper, the flow conditions will be referred to by their respective Run numbers as given in Table 1 and Fig. 3. Table 1 provides important information for the flow conditions. In the table, j_c and j_d are the superficial velocities for the continuous and dispersed phases, respectively. The channel Reynolds number for any phase k is defined as,

$$Re_k = \frac{\rho_k j_k D_h}{\mu_k}. \quad (14)$$

Local data have been obtained using multi-sensor conductivity probes at two different axial locations corresponding to $L/D_h \sim 30$

Table 1
Flow conditions for data acquisition in the 25 mm ID test section.

Run	j_{c1} (m/s)	j_{c2} (m/s)	j_c (m/s)	j_d (m/s)	Re_c (–)	Re_d (–)	Re_d/Re_c (–)	$\Delta P_f/\Delta P_g$ (–)
2	0.121	0.094	0.215	0.012	5460	44	0.008	0.005
3	0.262	0.094	0.356	0.012	9011	44	0.005	0.010
4	0.115	0.094	0.209	0.050	5302	176	0.033	0.005
5	0.249	0.094	0.343	0.050	8696	176	0.020	0.014
6	0.124	0.094	0.218	0.112	5531	395	0.071	0.007
7	0.211	0.094	0.305	0.112	7733	395	0.051	0.020
8	0.402	0.093	0.496	0.056	12563	198	0.016	0.040
9	0.402	0.093	0.496	0.112	12563	395	0.031	0.040
10	0.651	0.093	0.745	0.056	18877	198	0.010	0.080
11	0.649	0.093	0.742	0.112	18814	395	0.021	0.070

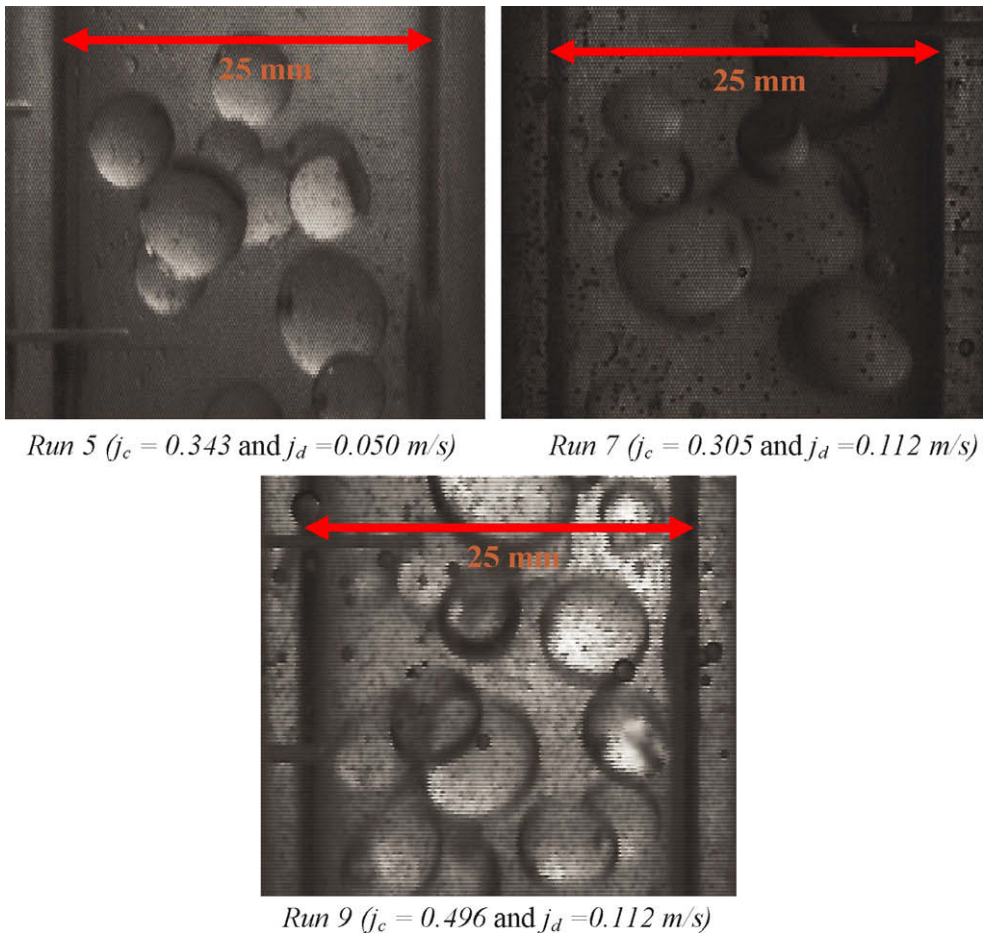

Fig. 2. Characteristic images for Runs 5, 7 and 9 taken at an $L/D_h \sim 42$ (Note that the small dots in the images are gas bubbles in the water box surrounding the test section. The images have been processed using Adobe Photoshop® to improve their quality).

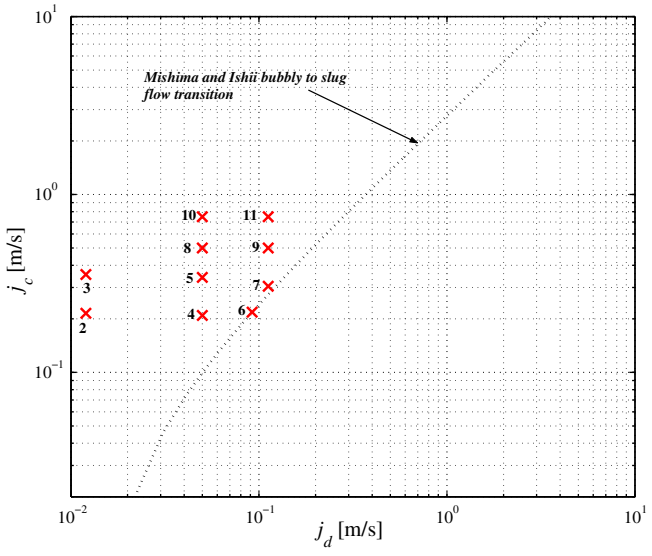

Fig. 3. Flow conditions in Table 1 on a flow pattern map.

and 58 (Vasavada et al., 2007). Data was acquired at 11 radial location at each axial measurement location for all 10 flow conditions. A particular two-phase flow parameter at each local data point is weighed with its corresponding radial location and a third order polynomial fit to these "weighted" datapoints is integrated to yield the area-averaged value for that parameter. Detailed analysis of the radial and axial variations of the two-phase flow parameters acquired show the presence of coalescence mechanism (Vasavada et al., 2007).

Vasavada et al. (2007) hypothesized that this coalescence was mainly driven by turbulence in the continuous phase based on the fact that the other potentially significant coalescence mechanism (wake entrainment) depends on the relative velocity, as is evident from Eq. (9), which is expected to be small for reduced-gravity two-phase flows on account of the reduction in buoyancy. This small averaged relative velocity (between 3 and 6 cm/s) was also observed from the current experimental data. A similar hypothesis has also been made by other researchers (Kamp et al., 2001). During the evaluation of the dominant mechanisms for the change of interfacial area concentration, it was found that the above hypothesis is not completely accurate. This interesting conclusion will be discussed in the succeeding section.

The coalescence mechanism observed from the experimental data appeared to be enhanced on increasing the dispersed phase flowrate, and consequently the corresponding superficial velocity, while keeping the continuous phase flowrate constant. On the other hand, increasing the continuous phase flowrate for the same dispersed phase flowrate was also found to have the same effect although a "saturation" was reached beyond which an increase in the continuous phase flowrate did not contribute to coalescence. This was attributed to the decrease in the interaction time available between colliding drops (Vasavada et al., 2007). The size of drops for some of the flow conditions in which this "saturation"

was observed, e.g., in Runs 8 and 9, may also be a factor leading to this behavior because if the drop size is larger than the size of the largest eddy, turbulence is no longer effective at driving drop coalescence. It is to be noted that in the formulation of the random collision mechanism used in the IATE and also in similar models developed by other researchers, e.g. (Tsouris and Tavlarides, 1994; Prince and Blanch (1990)), the basic assumption is that eddies of the same size as the bubbles and drops drive the interaction mechanism. In the next section details regarding the evaluation strategy for comparing the results of the IATE predection against our experimental data are provided as well as a critical discussion of the results.

4. IATE model evaluation

4.1. Evaluation strategy

The evaluation strategy involved using the one-group one-dimensional IATE that has been developed for normal-gravity air–water upflow in pipes and evaluated against relevant data from 12.7, 25 and 50 mm ID channels. This approach was taken in order to determine the applicability of each of the interaction mechanisms present therein for reduced-gravity flows. Certain technical details regarding the evaluation are worth discussing here.

The drop velocity, $\langle\langle v_{dz}\rangle\rangle$, and void fraction are unknowns in the field equations of the two-fluid model. Therefore, to obtain the exact solution of the interfacial area concentration from this equation, the field equations should be solved in a coupled manner together with the IATE. However, this approach will make the present evaluation more complicated and also introduce other uncertainties that may result from the interfacial drag constitutive relations. In view of this, a simplified approach is necessary. One approach is to replace the momentum equation with the drift-flux model. The one-dimensional drift-flux model can written as, (Zuber and Findlay, 1965):

$$\langle\langle v_d\rangle\rangle = \frac{\langle j_d\rangle}{\langle\alpha\rangle} = \left[\frac{\langle\alpha j\rangle}{\langle\alpha\rangle\langle j\rangle}\right]\langle j\rangle + \frac{\langle\alpha V_{dj}\rangle}{\langle\alpha\rangle} = C_0\langle j\rangle + \langle\langle V_{dj}\rangle\rangle, \tag{15}$$

where, C_0 is the distribution parameter and $\langle\langle V_{dj}\rangle\rangle$ is the void-weighted drift velocity.

It should also be mentioned that $\langle\langle v_{dz}\rangle\rangle$ for each flow condition is also available directly from the experimental data using area-averaging. In the present study, these experimental values are used in the IATE evaluation to eliminate any unquantifiable uncertainity introduced otherwise. Results using $\langle\langle v_{dz}\rangle\rangle$ obtained from the drift-flux approximation, which is ultimately based on experimental data, showed no major differences.

Furthermore, the turbulent velocity u_t used for normal-gravity IATE evaluation is given by the following relation (Batchelor, 1951),

$$u_t = 1.4(\epsilon D_b)^{\frac{1}{3}}, \tag{16}$$

where, ϵ is the turbulent kinetic energy dissipation rate per unit mixture mass for two-phase flow. It should be noted that the relation given in Eq. (16) is valid in the inertial subrange. As pointed out in the previous section, local data analysis showed that for some flow conditions the drop sizes were larger than the largest eddy size calculated as (Pope, 2000),

$$D_e = \frac{\kappa D_h}{2}, \tag{17}$$

where, κ is the von-Karman constant and is taken as 0.41 for pipe flows (Pope, 2000). For these cases, the assumption made during the modeling of the random collision process, that the bubbles/drops lie in the inertial subrange, appears to be invalid. However, Risso and Fabre (1998) have shown that such bubbles/drops also lie in the intertial subrange. Hence, the assumption in random collision mechanism may be valid for most of the flow conditions considered here. It should be noted that to determine the turbulent dissipation, ϵ, required to calculate the turbulent fluctuating velocity, a detailed model like the $k-\epsilon$ model may be used. However in this study, a simple algebraic correlation given as,

$$\epsilon = f_{TW}\frac{\langle v_m\rangle^3}{2D_h} \tag{18}$$

was employed, where, f_{TW} is the two-phase frictional factor and $\langle v_m\rangle$ is the mixture velocity. This model basically assumes that all the turbulence produced at the wall (due to the frictional pressure gradient) will be dissipated in the continuous phase. This assumption implies that the transport of eddies formed at the wall is unhindered by the dispersed phase. It is evident from the analyses and profiles of the local void fraction, shown in Vasavada et al. (2007), that the drops are distributed fairly uniformly across the channel. Although wall peaking is observed for some flow conditions, it is not as severe as in the case of normal-gravity air–water flow. Similar observations regarding the distribution of bubbles in air–water flows in reduced-gravity conditions have been made by other researchers (Colin et al., 1993; Kamp et al., 1995). Therefore, the assumption being made in the approximation for turbulent dissipation given by Eq. (18) is valid, in general, for reduced-gravity two-phase flows. The experimental results provide a stronger basis for the validity of the above assumption over a larger range of flow conditions in reduced-gravity conditions as compared to normal-gravity case.

The adjustable coefficients C_{TI}, C_{RC}, and C_{WE} account for proportionalities and assumptions in modeling the respective interaction mechanisms. They also need to be specified based on the experimental data in order to evaluate the model. The current study employed the same coefficients, except for α_{max}, as used for normal-gravity air–water two-phase flows. These are given as (Wu et al., 1998),

$$C_{RC} = 0.0021, C = 3.0, \alpha_{max} = 0.52 C_{WE} = 0.002,$$
$$C_{TI} = 0.034, We_{cr} = 6.0 \tag{19}$$

The maximum void fraction (or "packing") given by α_{max} was changed from the normal-gravity value to account for the large size of drops present in the current experiments and representative of reduced-gravity two-phase flows (as explained earlier using scaling). For normal-gravity cases the value of 0.741 was used for α_{max} whereas simple geometric consideration using the maximum spherical drop size for the present case (10 mm) gave a value of 0.52. The expansion term in the one-group one-dimensional IATE, given in Eq. (10), is set to zero during evaluation. For the current case this is valid since the experiments have been carried out using incompressible liquids. However, this condition is also expected to hold for actual gas–liquid two-phase flows in reduced-gravity conditions for cases where inertia and hence frictional pressure gradient is not dominant.

Before presenting and discussing the results of the IATE evaluation we would like to comment on the adjustable coefficients that appear in the IATE. The presence of 4 adjustable coefficients, viz. $C_{RC}, C, C_{WE}, C_{TI}$, in the one-group one-dimensional IATE may make interested readers skeptical about the usefulness of the model itself. While the authors of this paper concede that the presence of experimentally adjustable coefficients is not ideal, their presence is, at present, unavoidable on account of the complexity of modeling local interactions and their outcome across a variety of flow conditions and fluid properties. Although a body of literature exists dealing with the local mechanics of binary collisions between drops and bubbles, no clear extension of these results to a multi-

particle system and an averaged approach is available. It should be noted that, especially for the IATE presented here, the results of the local studies have been incorporated in the model wherever appropriate (e.g. for the minimum film thickness and interaction times in random collision based coalescence, see Hibiki and Ishii (2000) for details).

A simple numerical approach using a finite differencing method was applied to solve Eq. (12) in the model benchmarking process. The measured values of the interfacial area concentration and void fraction at the lowest measurement location ($L/D_h \sim 30$), and the superficial velocities of the continuous and dispersed phases served as the boundary conditions.

4.2. Results of evaluation

The results from the evaluation of the one-dimensional one-group IATE against experimental data corresponding to Runs 2 through 11 are provided here.

Figs. 4–6 show the results of the evaluation wherein the symbols indicate the measured area-averaged interfacial area concentration, $\langle a_i \rangle$, and the line represents the prediction made by the IATE at each spatial advance of the numerical algorithm. The error bars in Figs. 4–6 are representative of ±15%. As discussed in Vasavada et al. (2007), the calibration of the conductivity probe for the current experiments gave an error of ±12% for the local interfacial area concentration. The area-averaging scheme used to derive area-averaged parameters from the local values introduces further errors which are not easily quantifiable. Therefore, the addition of ±3% error to the local error in the measurement of a_i is somewhat arbitrary. Fig. 7 shows the percentage error between the predicted and measured interfacial area concentration at the final axial location ($L/D_h \sim 58$) for each of the flow conditions considered. The error depicted therein is calculated as,

$$Error = \left\{ \frac{(a_{ip} - a_{im})}{a_{im}} \right\} \times 100\% \qquad (20)$$

where, a_{im} and a_{ip} represent the experimentally measured and predicted interfacial area concentration, respectively.

As can be observed from Figs. 4–7 the prediction of the unmodified IATE is good with the maximum error for these flow conditions being 22% for Run 11. The dominant mechanisms existing in each of these flow conditions as per the IATE prediction are

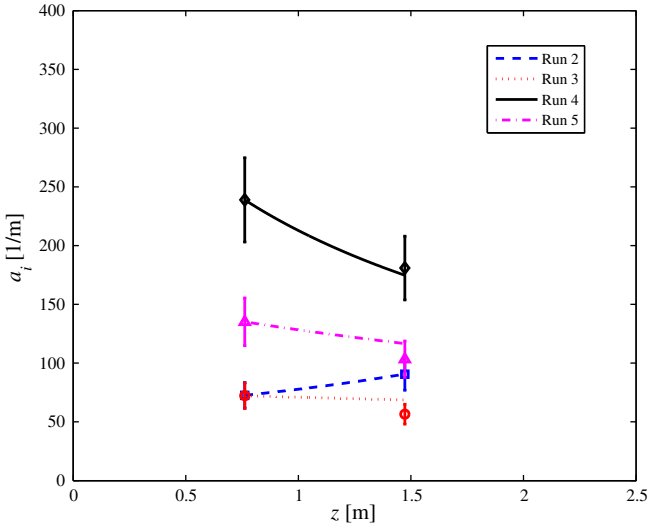

Fig. 4. Comparison of predictions of one-dimensional one-group IATE against experimental data for Runs 2, 3, 4 and 5.

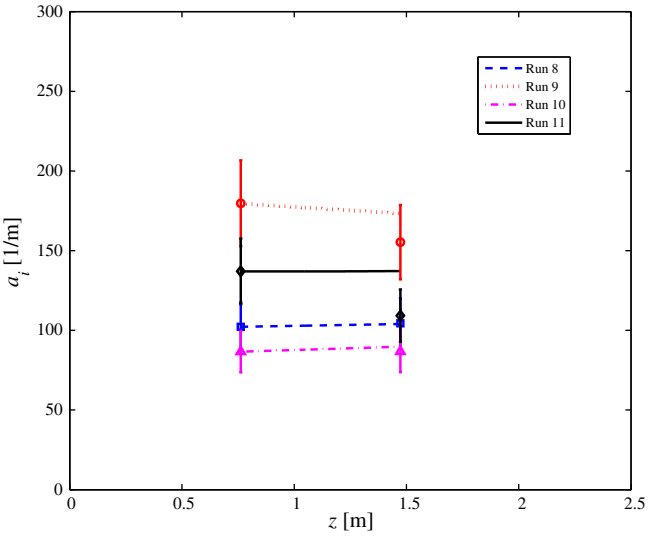

Fig. 5. Comparison of predictions of one-dimensional one-group IATE against experimental data for Runs 8, 9, 10 and 11.

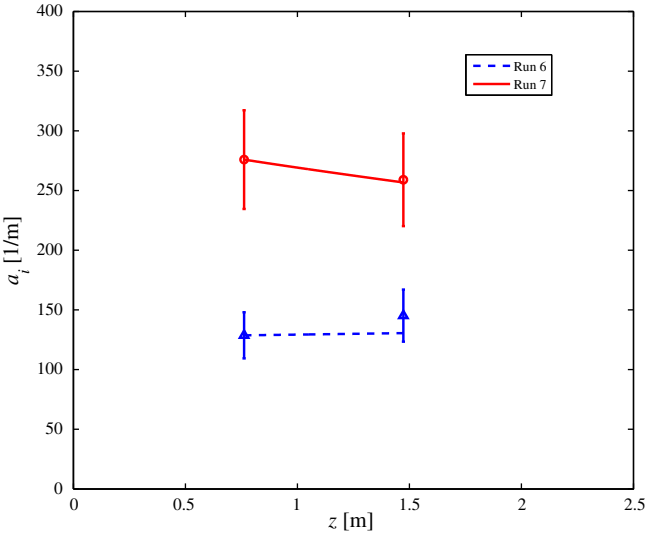

Fig. 6. Comparison of predictions of one-dimensional one-group IATE against experimental data for Runs 6 and 7.

the random collision and wake entrainment based coalescence. The contribution of each of these to the change in the interfacial area concentration for different flow conditions is shown in Figs. 8–13. The figures show the contribution of random collision based coalescence for different flow conditions followed by the contribution of wake entrainment for the same flow conditions. Further, the figures show flow conditions for which either the continuous or dispersed phase superficial velocity increases keeping the other the same. Wake entrainment mechanism is seen to be more important as compared to random collision for some of the flow conditions most notably the ones with low j_c and j_d. This is clearly evident from a comparison of the relative contribution of these mechanisms for Runs 2, 3 and 4. The contribution from wake entrainment is appreciably higher as compared to random collision for these flow conditions. However, the contribution of random collision appears on par with wake entrainment as the continuous and or dispersed phase superficial velocities are increased. This can be seen from Figs. 10 and 11 where the contribution of random collision increases from Run 4 to Run 10 where is becomes similar to

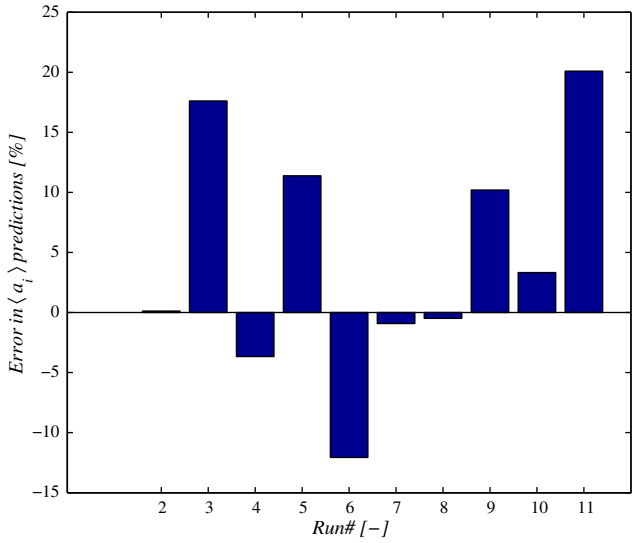

Fig. 7. Relative error of the interfacial area concentration ($\langle a_i \rangle$) between experimental data and predictions by one-dimensional one-group IATE.

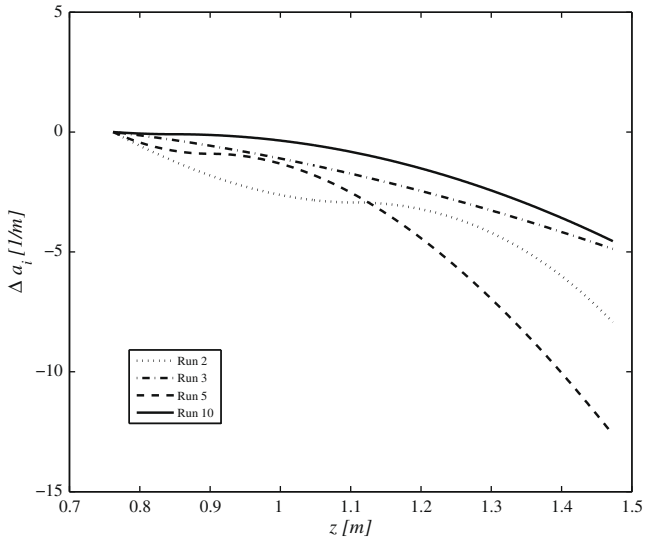

Fig. 9. Contribution of wake entrainment mechanism to change in interfacial area concentration($\langle a_i \rangle$) for Runs 2, 3, 5 and 10.

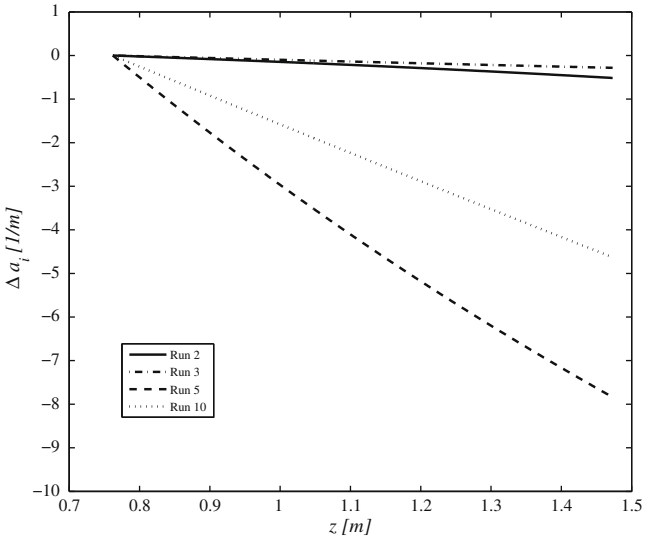

Fig. 8. Contribution of random collision mechanism to change in interfacial area concentration($\langle a_i \rangle$) for Runs 2, 3, 5 and 10.

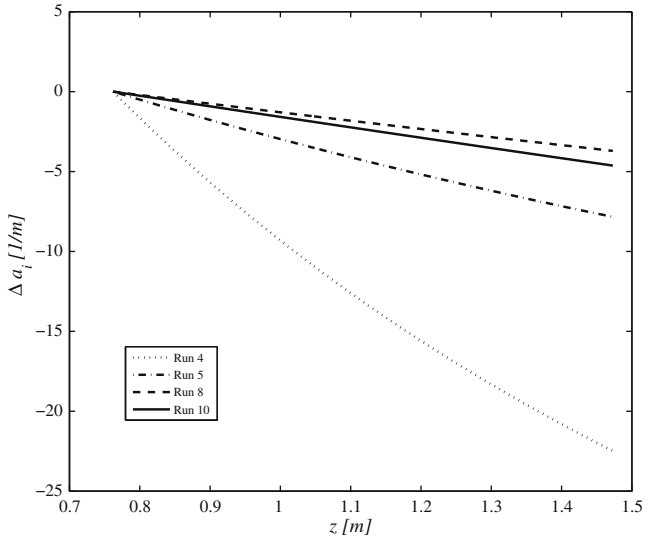

Fig. 10. Contribution of random collision mechanism to change in interfacial area concentration($\langle a_i \rangle$) for Runs 4, 5, 8 and 10.

wake entrainment. This is further evident from Figs. 12 and 13. It should be noted that the very low contribution of either of these mechanisms to Run 11 is on account of the reduced interaction time available as commented on in Vasavada et al. (2007).

4.3. Discussion of results

A critical discussion of the results shown in the previous section and their interpretation is presented in the following paragraphs as well as in the next sub-section. To put the ensuing discussion in proper perspective, it is worthwhile to reiterate the primary goal of the present work, which is to develop a predictive model for reduced-gravity two-phase bubbly flow development. Therefore, although the model predicts the current experimental data well, the discussion is aimed at explaining the predictions with the hypothesis that actual reduced gravity two-phase flow systems will, most likely, be gas–liquid systems.

It is interesting to note that the contribution of coalescence due to wake entrainment is important for reduced-gravity conditions also, especially at low continuous phase velocities where random collision driven by turbulent eddies is not significant. As the continuous and/or dispersed phase superficial velocities are increased, thereby increasing the turbulence in the flow, random collision driven coalescence starts to become important. As we move closer to the transition from bubbly to slug flow, random collision driven coalescence becomes dominant over wake entrainment. It should be noted that increasing the continuous and/or dispersed phase superficial velocity causes an increase in the turbulence generated at the wall as well as the bubble induced turbulence.

For reduced-gravity conditions, Kamp et al. (2001) have assumed that due to the small relative velocity at such conditions, the wake induced collisions will be nearly absent. Although the state of the dispersed phase in air–water experiments at normal and reduced-gravity is different, the above results were obtained using the normal-gravity IATE developed for air–water flows without any modifications to the mechanisms or adjustable coefficients. Hence, the model does not "know" about the differences

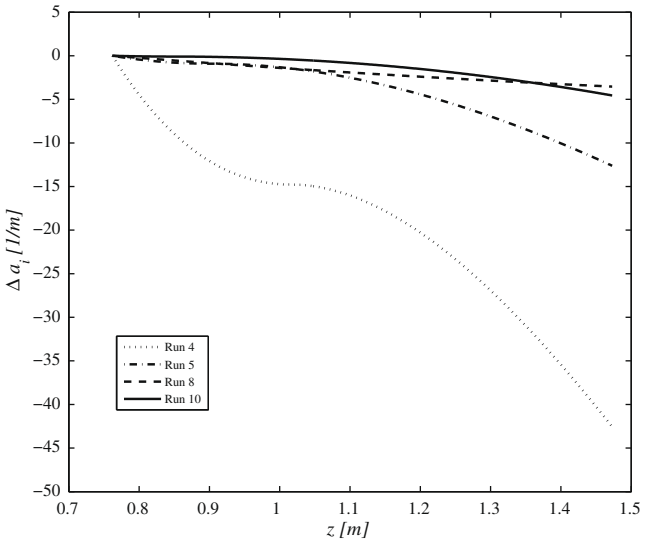

Fig. 11. Contribution of wake entrainment mechanism to change in interfacial area concentration($\langle a_i \rangle$) for Runs 4, 5, 8 and 10.

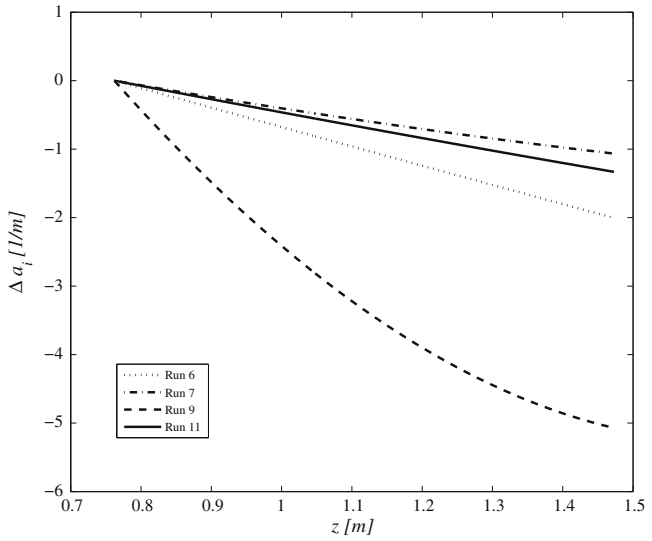

Fig. 13. Contribution of wake entrainment mechanism to change in interfacial area concentration($\langle a_i \rangle$) for Runs 6, 7, 9 and 11.

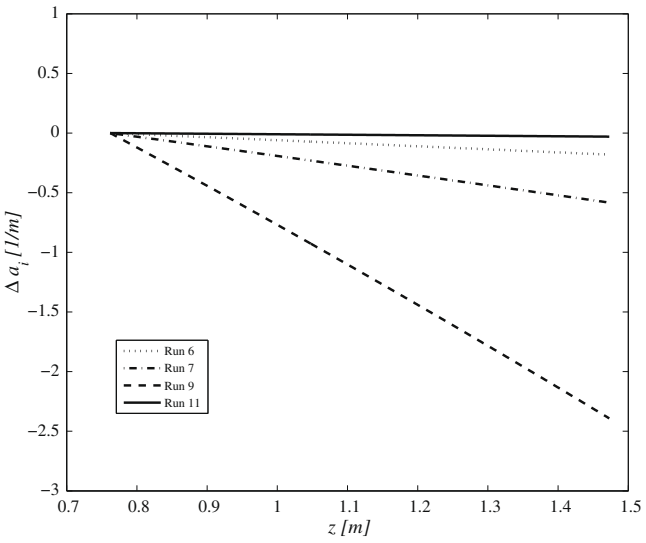

Fig. 12. Contribution of random collision mechanism to change in interfacial area concentration($\langle a_i \rangle$) for Runs 6, 7, 9 and 11.

in the dispersed phase. Further discussion of the differences in the interaction phenomena in drops and bubbles as well as the influence of differences in dispersed phase properties will be discussed in the next sub-section. However, there are physically valid reasons for the results of the model and these arguments will be put forth hereunder.

It is known that the presence of the dispersed phase flattens the single-phase velocity profile and also the distribution of turbulent intensity, which is a measure of the strength of turbulent fluctuations (Lance and Bataille, 1991; deBertodano et al., 1994). Moreover, in reduced-gravity conditions, the distribution of the void fraction is fairly uniform across the test section, especially for flow conditions with low continuous and dispersed phase velocities, as opposed to the center peak or wall peak profile often seen in the normal-gravity gas–liquid two-phase flows (Vasavada et al., 2007). This uniform distribution of the void causes the turbulent eddies, formed at the wall, to lose a major portion of their energy as they diffuse towards the center of the pipe/channel. In addition to this, as argued by Kamp et al. (1995), since the drops/bubbles at reduced-gravity conditions remain spherical in spite of their large sizes, they can absorb much of the energy of the eddies, which will consequently not be available for driving the collision process.

As opposed to this, as the continuous and/or dispersed phase superficial velocities are increased, a center peaked profile starts to appear due to coalescence especially in the transition region from bubbly to slug flow. In such cases, the arguments laid forth in the previous paragraph do not remain entirely valid and therefore random collision becomes an important interaction mechanism. The data acquired and used for validation by Kamp et al. (2001) lies in the high Reynolds number region for the continuous phase ($Re_c \sim 66,000$ to $88,000$). Therefore, random collision at such high values of Re_c will dominate over the wake entrainment whereas the same argument will not always be true in the present study since Re_c ranges from $\sim$ 5000 to 19,000 here. Evidence pointing in this direction can be obtained from the turbulent dissipation rate ϵ, which in turn determines the turbulent fluctuating velocity, which acts as the driving force for bubble/droplet collision. In the current study ϵ is an order of magnitude lower for some of the flow conditions being discussed as compared to those of Kamp et al. (1995).[2] The maximum turbulent dissipation for the flow conditions under discussion is for Run 11 ($\epsilon \sim 0.4 \mathrm{m}^2/\mathrm{s}^3$) as opposed to 1.15 for Kamp et al. (1995). As mentioned earlier, Kamp et al. (1995) have ruled out the possibility of wake entrainment based coalescence without an analysis and only on the basis that the relative velocity is small in reduced-gravity conditions. This premise also needs to be examined quantitatively.

The relative velocity for the flow conditions being considered obtained from the area-averaged values of experimental data at the highest axial location ($L/D_h \sim 58$) are listed in Table 2. The predicted values of the droplet Sauter mean diameter at the axial location of $L/D_h \sim 58$ compared favorably against those obtained from the area-averaging of the local data at the same measurement location as shown in Fig. 14. Using the relative velocity and the Sauter mean diameter calculated from the IATE, the particle Reynolds number, given as,

[2] In these calculations, the turbulent energy dissipation rate for each case was determined using Eq. (18) with the respective pressure drop values. It is assumed in both cases that all the turbulence produced at the wall is dissipated in the continuous phase. As mentioned, this may not be entirely true for reduced-gravity conditions.

$$Re_p = \frac{\rho_c u_r D_b}{\mu_c}, \tag{21}$$

can be calculated. In the above equation, the droplet Sauter mean diameter D_{sm} is used in place of D_b. In the current case, since the drops are spherical in almost test runs, there is no distinction, physically or otherwise, between D_{sm} and D_b. It should be noted that the above equation does not distinguish between the state of the dispersed phase and hence the results and discussion are applicable to both bubbles and drops. The particle Reynolds number is the measure of the relative force "seen" (or "experienced") by a bubble/drop as it moves in the continuous phase. If the continuous phase is in motion, the bubble/drop will experience a force only due to the relative velocity. Results of the calculation are tabulated in Table 2.

The particle (in the present case, droplet) Reynolds number for the current experimental conditions range from ~ 50 for Run 10 to $\sim$1700 for Run 6. It is well known (Clift et al., 1978; Ishii and Zuber, 1979) that beyond a particle Reynolds number of 1, wakes are formed behind the particle and the separation and length of wakes increases with the particle Reynolds number. For the range of particle Reynolds numbers calculated here, there is strong basis for the presence of wakes. Referring to Table 2, the relative velocity predicted by the IATE is not large as compared to normal-gravity two-phase flows, where even spherical/distorted bubbles have a terminal velocity of about 0.2 m/s in air–water flows at atmospheric conditions. However, despite the small relative velocity in reduced-gravity conditions, the particle Reynolds number is large enough to activate the wake entrainment mechanism. This is on account of the fact that the size of the particles is significantly large as compared to normal-gravity two-phase flows (such a comparison has been made in Vasavada et al. (2007)). For an air bubble 5 mm in diameter (or Sauter mean diameter) and moving through water with a relative velocity of 0.03 m/s, using Eq. (21) gives $Re_p \sim 150$ and the particle lies in the wake regime. Numerical simulations by Dandy and Leal (1989) for drops and Ryskin and Leal (1984) for bubbles also support this assertion. Some differences do exist, as per the numerical results of Dandy and Leal (1989) and Ryskin and Leal (1984) regarding the shape of bubbles and drops required for wakes to form. This difference will be pointed out and discussed in the next sub-section.

Moreover, Tomiyama et al. (1998) and Takamasa et al. (2004) have also pointed to the presence of a small but finite relative velocity at reduced-gravity conditions. Takamasa et al. (2004) have given an analytical expression comparing the relative velocity to be expected in the reduced-gravity conditions to that at the normal-gravity conditions for same continuous phase Reynolds number (Re_c). The result obtained for an air–water system at $0.03g_e$ using the relation given by Takamasa et al. (2004) is shown in Fig. 15. The use of this relation for the present case yielded relative velocities that are similar to those obtained experimentally as well as

Table 2
Relative velocity determined at $L/D_h \sim 58$ from experimental data.

Run	Relative Velocity (m/s)	Re_p (–)
2	~0.025	~80
3	~0.024	~100
4	~0.060	~280
5	~0.055	~300
6	~0.15	~1700
7	~0.019	~100
8	~0.0125	~80
9	~0.0075	~280
10	~0.0010	~50
11	~0.070	~250

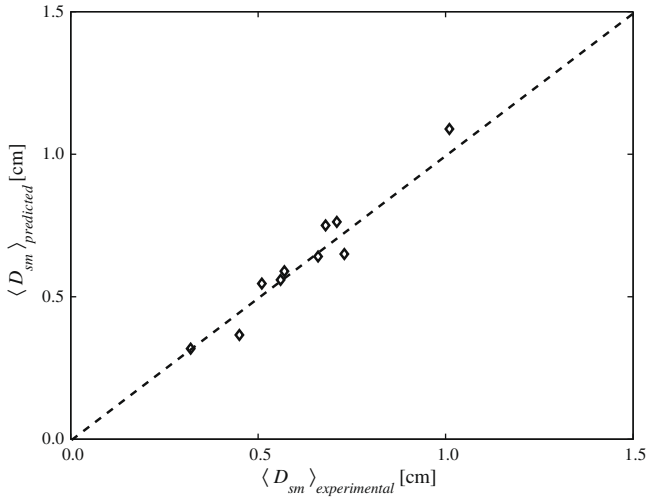

Fig. 14. Comparison of averaged droplet Sauter mean diameter ($\langle D_{sm} \rangle$) predicted by the one-dimensional one-group IATE against that obtained from local measurements for Runs 2 through 11.

using the IATE. It is evident from Fig. 15 that even for reduced-gravity conditions, the presence of the relative velocity cannot be neglected completely. Rezkallah and Nakazawa (1997) contend that the relative velocity for bubbly flows at reduced-gravity conditions is very small and can be neglected. The results and analysis presented above indicate that even for low relative velocities, which will exist in reduced-gravity conditions, the existence of wake entrainment cannot be overlooked. As stated previously, Takamasa et al. (2003) have shown that the IATE developed for normal-gravity condition predicts their experimental data well with wake entrainment being the dominant interaction mechanism. They believe that the velocity profile induced coalescence is the dominant mechanism since their flow conditions lie in the laminar and laminar to turbulent transition regions for the continuous phase. Takamasa et al. (2003) have attributed the agreement between the IATE predictions and their data to the similar behavior of wake entrainment and velocity profile induced coalescence mechanisms. Calculation of Re_p for their data reveals that this parameter takes values ranging from 60-120. Based on the above analysis, it is evident that wake entrainment is present. For the

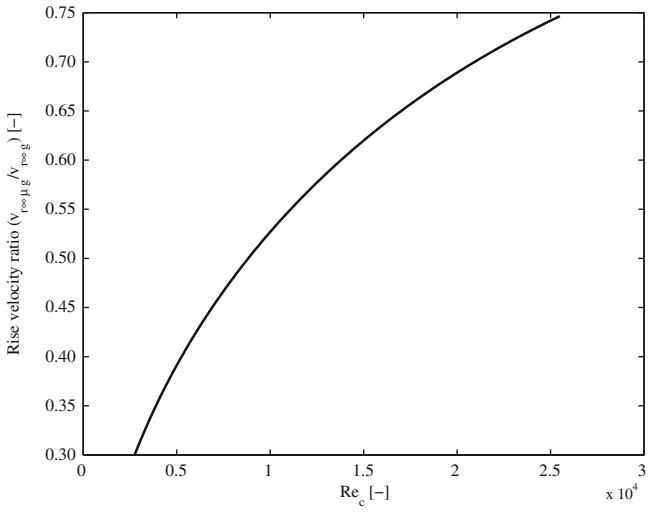

Fig. 15. Ratio of rise velocity of single bubble at $0.03g_e$ to the normal-gravity condition using the relation given by Takamasa et al. (2004).

flow conditions where the random collision based coalescence is not strong, wake entrainment is the dominant mechanism causing bubble/drop coalescence. It is also worth noting that Hibiki et al. (2006), using their drift-flux model, showed the existence of an appreciable relative velocity for the data of Takamasa et al. (2004).

4.4. Discussion of differences in fluid properties

It is well known that for flows with small Reynolds number, with undeformed fluid particle spheres, the Hadamard–Rybczynski theory is not obeyed in practice (Clift et al., 1978). This has been attributed, and confirmed through experiments, to the lack of internal circulation in the fluid spheres, in which case the external flow around the fluid spheres is indistinguishable from that around a solid sphere at the same Re_p. The lack of internal circulation in fluid particles can be traced to high viscosity ratio, μ_d/μ_c, or the presence of surface contaminants. It is due to the immobility of the interface in gas–liquid flows that wake structures are formed much like those behind spheres and the discussion and arguments put forth in the previous section remain valid. This is also the reason for Takamasa et al. (2003) observing wake entrainment as being dominant in bubble interactions at reduced-gravity conditions. Clift et al. (1978) also provide further results in favor of this claim. To quote Clift et al. (1978) regarding the effect of surface contaminants on the behavior of fluid particles (bubbles/drops),

> "Systems which exhibit high interfacial tensions, including common systems like air/water, liquid metals/air and aqueous liquids/nonpolar liquids, are most subject to this effect."
> "The measures required to purify such systems and the precautions needed to ensure no further contamination are so stringent that one must accept the presence of surface-active contaminants in most systems of practical importance."

Simulations by Dandy and Leal (1989) and Ryskin and Leal (1984) showed some differences in the requirement on bubble/drop shapes for generation of wakes which should be mentioned here. Dandy and Leal (1989) found that no deformation of the drops is necessary for a wake to be formed whereas according to Ryskin and Leal (1984) bubbles need to reach a "critical" deformation before wakes can be formed. Although flow visualization images in Kamp et al. (2001), Takamasa et al. (2003) and Lowe and Rezkallah (1999) as well as simulations results of Clarke and Rezkallah (2001) do show deformed bubbles, it is reasonable to assume that the structure of bubbles will be similar to those observed for the drops in the current experiments for the same flow conditions. In this case too, the fact that in any practical system, fluid particles (bubbles/drops) will behave akin to solid particles, in as much as the immobility (although partial) of the interface, will cause wake formation behind bubbles even if they are not significantly distorted.

Two important differences between the current experiments and an actual gas–liquid system in reduced-gravity conditions are the density and viscosity of the dispersed phase, two and three orders of magnitude higher, respectively, in the present study as compared to air. Each of these need to be considered in light of the interaction mechanisms. The turbulent eddies will have to expend more energy to bring about a collision event between two drops due to their higher inertia as compared to air bubbles. The higher density and viscosity of droplets will also decrease the occurrance of breakup by turbulent eddies since again the eddies will have to spend more energy to break up the drops and further, the higher viscosity will help damp out some of the interfacial oscillations which contribute to the breakup of bubbles/drops (Risso and Fabre, 1998). To examine the effect of the higher density of drops compared to air bubbles, the turbulent fluctuating velocity given in Eq. (16) was modified by including a term involving the density ratio between the continuous and dispersed "phases". The resulting expression is given as,

$$u_t = 1.4(\epsilon D_b)^{\frac{1}{3}}\sqrt{\frac{\rho_c}{\rho_c+\rho_d}}, \tag{22}$$

accounting for the fact that for inertial terms, the velocity scales as the square root of the density. The results from the IATE with the above modification were not significantly different from those presented here. The increased density will also decrease the acceleration of drops entrained in wakes of preceeding drops. However, no modifications have been made to any mechanism in the final IATE developed for reduced-gravity two-phase flows. This is because the IATE has shown the ability to predict the change in $\langle a_i \rangle$ for the present case as well as the air–water data of Takamasa et al. (2003), thereby proving its general applicability. Moreover, the change in the errors of IATE prediction on account of any modification to the mechanisms cannot be evaluated critically because the errors in prediction by the unmodified IATE are within the experimental uncertainities. Changes of predictive errors in this range are not meaningful since the experimental values of $\langle a_i \rangle$, which are used as reference, also contain uncertainities in that range.

Roig and Tournemine (2007) recently reported the results of their measurements of the local liquid velocity between bubble swarms (termed "interstitial velocity" by them) using conditional averaging. They mention that as the void fraction increases it becomes increasingly difficult to separate the influence of the surrounding bubbles on the continuous phase. The results of Roig and Tournemine (2007) provide further evidence for our claim of the presence of wakes based on Re_p and the rigid particle like behavior of bubbles/drops. They report the existence of wakes for air bubbles with an average diameter of 2 mm and with a relative velocity of 0.25 m/s which corresponds to Re_p of ~40. Moreover, they also find that increasing the void fraction (in their case up to 13%) caused a decrease in the wake length from ~8 to ~3 times the bubble diameter. It should be noted that in modeling the wake interaction mechanism in the one-group IATE, the wake length has been assumed to be ~5 times the bubble diameter.

5. Summary

The one-group IATE, applicable to bubbly flows, has the ability to predict the change of the interfacial area concentration in application with the two-fluid model. Detailed experiments were carried out in a 25 mm ID ground-based test section wherein a reduced-gravity condition was simulated using two immiscible liquids of similar density. Based on detailed analysis of experimental data, the dominant fluid particle interaction mechanisms were identified. The one-dimensional one-group IATE developed for normal-gravity conditions was evaluated against the acquired data. The predictions of the IATE were analyzed in light of the physics of two-phase flow and differences in fluid properties. The salient details of the evaluation and interpretation of results are listed hereunder.

- The one-dimensional one-group interfacial area transport equation was evaluated based on the acquired data in order to determine its applicability and predictive ability for reduced-gravity two-phase flows. The area-averaged two-phase flow parameters derived from the local data at different axial locations were used in this analysis. The one-dimensional one-group IATE used for normal-gravity conditions was used without any major changes to the models or coefficients. Only the maximum void fraction was modified to account for larger drop/bubble sizes in reduced-gravity conditions.

- Flow conditions lying in the bubbly and bubbly to slug transition flow regime were used for evaluation purposes and a systematic approach was undertaken to validate the different interaction mechanisms.
- Flow conditions in the bubbly flow regime, where coalescence was expected to dominate, were used to evaluate the available models and relative strength of coalescence due to random collision and wake entrainment mechanisms. These mechanisms were identified as dominant ones in the local data analysis. The maximum error between the prediction and experimental data for the area-averaged interfacial area concentration in the ten rest runs was found to be 22%.
- From this analysis it was found that wake entrainment had a stronger effect as compared to random collision for flow conditions with low continuous and/or dispersed phase superficial velocity. As the superficial velocities of either phase, and therefore the turbulence in the flow, increase random collision becomes dominant over wake entrainment. Wake entrainment based coalescence was not expected since the relative velocity was found to be small (an order of magnitude smaller than that for normal-gravity air–water flow). However, the large size of the drops (on account of the reduction in the density difference) resulted in fairly large droplet Reynolds numbers, which lie in the wake regime. This leads to the formation of wakes and the presence of wake entrainment based coalescence.
- The comparisons showed that the modeled interaction mechanisms existing in the one-dimensional one-group IATE are physically sound. Moreover, they have been shown to represent the physics existing in reduced-gravity two-phase flows for the flow conditions considered here. This study demonstrates the ability of the IATE to model the evolution of two-phase bubbly flows in reduced-gravity conditions.

Acknowledgements

This work was supported by the National Aeronautics and Space Administration (NASA), Office of Biological and Physical Research under grant NNC04GA26G administered by the NASA Glenn Research Center, Cleveland, OH. The authors thank Dr. Fran Chiaramonte of the NASA Glenn Reserach Center for his support of this work. The authors also acknowledge Dr. Y. Mi of En'urga Inc., West Lafayette, IN for his help with the instrumentation.

Appendix A. Supplementary data

Supplementary data associated with this article can be found, in the online version, at doi:10.1016/j.ijmultiphaseflow.2009.01.006.

References

Batchelor, G., 1951. Pressure fluctuations in isotropic turbulence. In: Proceedings of Cambridge Philosophical Society. No.47. Cambridge, UK, pp. 359–371.
Clarke, N., Rezkallah, K., 2001. A study of drift velocity in bubbly two-phase flow under microgravity conditions. Int. J. Multiphase Flow 27 (9), 1533–1554.
Clift, R., Grace, J., Weber, M., 1978. Bubbles, Drops and Particles. Academic Press.
Colin, C., Fabre, J., Dukler, A., 1991. Gas–liquid flow at microgravity conditions -I: dispersed bubble and slug flow. Int. J. Multiphase Flow 17, 533–544.
Colin, C., Fabre, J., Dukler, A., 1993. Influence of gravity on void and velocity distribution in two-phase gas–liquid flow in pipe. Adv. Space Res. 7, 141–145.
Colin, C., Fabre, J., Dukler, A., 1996. Bubble and slug flow at microgravity conditions: state of knowledge and open questions. Chem. Eng. Commun. 141–142, 155–173.
Dandy, D., Leal, L., 1989. Buoyancy-driven motion of a deformable drop through a quiescent liquid at intermediate Reynolds numbers. J. Fluid Mech. 208, 161–192.
deBertodano, M.L., Jones, O., 1994. Phase distribution in bubbly two-phase flow in vertical ducts. IJMF 20 (5), 805–818.
Dukler, A., Fabre, J., McQuillen, J., Vernon, R., 1988. Gas–liquid flow at microgravity conditions: flow patterns and their transitions. Int. J. Multiphase Flow 14, 389–400.
Fu, X., 2001. Interfacial area measurement and transport modeling in air–water two-phase flow. Ph.D. Thesis, Purdue University, West Lafayette, IN, USA.
Govier, G.K., Aziz, K., 1972. The flow of complex mixtures in pipes. Van Nostrand Reinhold Co., New York.
Grigoriev, Y., Grogorov, E., Cykhotsky, V., Prokhorov, Y., Gorbenco, G., Blinkov, V., Teniakov, I., Malukihin, C., 1996. Two-phase heat transport loop of central thermal control system for the International Space Station 'Alpha' Russian segment. AIChe Symp. Series-Heat Transfer 310, 9–17.
Hibiki, T., Ishii, M., 1999. Experimental study on interfacial area transport in bubbly two-phase flows. Int. J. Heat Mass Transfer 42, 3019–3035.
Hibiki, T., Ishii, M., 2000. One-group interfacial area transport of bubbly flows in vertical round tubes. Int. J. Heat Mass Transfer 43, 2711–2726.
Hibiki, T., Takamasa, T., Ishii, M., Gabriel, K., 2006. One-dimensional drift-flux model at reduced gravity conditions. AIAA J. 44 (7), 1635–1642.
Ishii, M., Hibiki, T., 2006. Thermo-fluid Dynamic Theory of Two-phase Flow. Springer, New York.
Ishii, M., Zuber, N., 1979. Drag coefficient and relative velocity in bubbly, droplet or particulate flows. AIChE J. 25 (5), 843–855.
Kamp, A., Chesters, A., Colin, C., Fabre, J., 2001. Bubble coalescence in turbulent flows: A mechanistic model for turbulence-induced coalescence applied to microgravity bubbly pipe flow. Int. J. Multiphase Flow 27, 1363–1396.
Kamp, A., Colin, C., Fabre, J., 1995. The local structure of a turbulent bubbly pipe flow under different gravity conditions. In: Proceedings of the Second International Conference on Multiphase Flow. No. P6-13. Kyoto, Japan.
Keshock, E., 1987. Two-phase flow tests conducted under normal and zero-gravity (KC-135 aircraft) conditions. Technical Report NAS9-17195, National Aeronautical and Space Administration.
Kim, S., 1999. Interfacial area transport equation and measurement of local interfacial characteristics. Ph.D. Thesis, Purdue University, West Lafayette, IN, USA.
Kim, S., Fu, X., Wang, X., Ishii, M., 2000. Development of the miniaturized four-sensor conductivity probe and the signal processing scheme. Int. J. Heat Mass Transfer 43, 4101–4118.
Kocamustafaogullari, G., Ishii, M., 1995. Foundation of the interfacial area transport equation and its closure relations. Int. J. Heat Mass Transfer 38, 481–493.
Lance, B., Bataille, J., 1991. Turbulence in the liquid phase of a uniform bubbly air–water flow. JFM 222, 95–118.
Lowe, D., Rezkallah, K., 1999. Flow regime identification in microgravity two-phase flows using void fraction signals. Int. J. Multiphase Flow 25, 433–457.
Mishima, K., Ishii, M., 1984. Flow regime transition criteria for upward two-phase flow in vertical tubes. Int. J. Heat Mass Transfer 27 (5), 723–737.
Pope, S., 2000. Turbulent Flows. Cambridge University Press, Cambridge, UK.
Prince, M., Blanch, H., 1990. Bubble coalescence and breakup in air-sparged bubble columns. AIChE J. 36 (10), 1485–1499.
Rezkallah, K., Nakazawa, N., 1997. A study of slip ratio in two-phase gas–liquid flow at normal and microgravity conditions. In: Proceedings of 1997 ASME Fluids Engineering Division Annual Summer Meeting.
Risso, F., Fabre, J., 1998. Oscillations and breakup of a bubble immersed in a turbulent field. JFM 372, 323–355.
Roig, V., Tournemine, A.L.D., 2007. Measurement of interstitial velocity of homogeneous bubbly flows at low to moderate void fraction. J. Fluid Mech 572, 87–110.
Ryskin, G., Leal, L., 1984. Large deformations of a bubble in axisymmetric steady flows Part. 2. The rising bubble. J. Fluid Mech. 148, 19–35.
Sun, X., 2001. Two-group interfacial area transport equation for a confined test section.
Sun, X., Kim, S., Ishii, M., Beus, S., 2004a. Model evaluation of two-group interfacial area transport equation for confined upward flow. Nucl. Eng. Design 230, 27–47.
Sun, X., Kim, S., Ishii, M., Beus, S., 2004b. Modeling of bubble coalescence and disintegration in confined upward two-phase flow. Nucl. Eng. Design 230, 3–26.
Takamasa, T., Hazuku, T., Fukamachi, N., Tamura, N., Hibiki, T., Ishii, M., 2004. Effect of gravity on axial development of bubbly flow at low liquid Reynolds number. Exp. Fluids 37, 631–644.
Takamasa, T., Iguchi, T., Hazuku, T., Hibiki, T., Ishii, M., 2003. Interfacial area transport of bubbly flow under microgravity environment. IJMF 29, 291–304.
Tomiyama, A., Kataoka, I., Zun, I., Sakaguchi, T., 1998. Drag coefficients of single bubbles under normal and micro gravity conditions. JSME Int. J. B 41 (2), 472–479.
Tsouris, C., Tavlarides, L., 1994. Breakage and coalescence models for drops in turbulent dispersions. AIChE J. 40, 395–406.
Vasavada, S., Sun, X., Ishii, M., Duval, W., 2007. Study of two-phase flows in reduced gravity using ground based experiments. Exp. Fluids 43, 53–75.
Wu, Q., Kim, S., Ishii, M., Beus, S., 1998. One-group interfacial area transport in vertical bubbly flow. Int. J. Heat Mass Transfer 41 (8–9), 1103–1112.
Zhao, J., Xie, J., Lin, H., Hu, W., Ivanov, A., Belyeav, A., 2001. Experimental studies on two-phase flow patterns aboard the MIR space station. Int. J. Multiphase Flow 27 (11), 1931–1944.
Zuber, N., Findlay, J., 1965. Average volumetric concentration in two-phase flow systems. J. Heat Transfer 87, 453–468.